Miscibility, Crystallization, and Mechanical Properties of Poly(3-hydroxybutyrate) and Poly(propylene carbonate) Biodegradable Blends

Dong Zhi Yang,[1] Ping Hu[2]

[1]*State Key Laboratory of Chemical Resource Engineering, College of Material Science and Engineering, Beijing University of Chemical Technology, Beijing 100029, China*
[2]*Department of Chemical Engineering, Institute of Polymer Materials and Engineering, Tsinghua University, Beijing 100084, China*

Received 7 August 2007; accepted 25 November 2007
DOI 10.1002/app.28002
Published online 23 April 2008 in Wiley InterScience (www.interscience.wiley.com).

ABSTRACT: Nine blends of poly(3-hydroxybutyrate) (PHB) and poly(propylene carbonate) (PPC), biodegradable polyester, and pure sample films were prepared with the ratio of PHB/PPC ranging from 90/10 to 10/90 by codissolving these two polyesters in chloroform and casting the mixture. The miscibility, crystallization, melting behavior, morphology, and mechanical properties of the blends have been studied by differential scanning calorimetry (DSC), Fourier transform infrared spectroscopy (FTIR), wide angle X-ray diffraction (WAXD), polarizing optical microscopy (POM), and scanning electron micrograph (SEM). The results indicated that PHB showed complete miscibility with PPC for PHB/PPC 30/70, 20/80, and 10/90, as evidenced by the only one composition-dependent glass transitions (T_g) of blends, and the T_gs close to the values calculated using the Fox equation. However, PHB showed immiscibility with PPC for the other six blends, as shown by the existence of almost unchanged T_g of PHB at about 2°C. According to the DSC analysis, the crystallization of PHB was suppressed by blending with abundant PPC. This result is consistent with results obtained from X-ray and POM results. Some interaction between the two macromolecules was confirmed by using FTIR analysis. SEM graphs showed that the blends containing PHB $\leq$ 30 wt % tend to form a more compact structure, and no obvious phase separation was found. The brittleness of PHB was improved apparently by blending with PPC. © 2008 Wiley Periodicals, Inc. J Appl Polym Sci 109: 1635–1642, 2008

Key words: poly(3-hydroxybutyrate); poly(propylene carbonate); blend miscibility; crystallization

INTRODUCTION

Bacterial poly(3-hydroxybutyrate) (PHB) is well known as a biodegradable thermoplastic polyester. It has many advantages such as biodegradability, biocompatibility, and optical activity.[1–3] The mechanical properties of PHB are very similar to those of polypropylene. However, the brittleness, high price, and poor thermal stability of PHB retard its commercial application.

An approach to improve the properties of PHB is to make miscible blends of PHB and another kind of polymer or plasticizer. So far, a variety of blends containing PHB have been studied, including binary blends with poly(vinyl acetate) (PVAc),[4,5] polymethyl methacrylate (PMMA),[6] poly(ethylene oxide) (PEO),[7–10] poly(vinyl alcohol) (PVA),[11] poly(butylene succinate) (PBSU),[12] poly(lactic acid) (PLA),[13,14] polycaprolactone (PCL),[15] poly(hydroxybutyrate-*co*-hydroxyvalerate) (PHBV),[16–18] poly(hydroxybutyrate-*co*-hydroxyhexanoate) [P(3HB-3HHx)],[19] and poly(epichlorohydrin) (PEP),[20] etc. In addition, the blends of polysaccharides, such as cellulose and starch derivatives, chitin, and chitosan, have also been reported.[21,22] Among these blends, PHB/PVAc,[4,5] PHB/PEO,[7] PHB/P(3HB-3HHx),[19] and PHB/PVA[11] systems were reported to be miscible over the whole composition range. The miscibility of PHB, PLA,[13] and PHBV[16–18] blends was dependent on the molecular weight of PLA and the fraction of HV unit, respectively. PHB/PMMA, PHB/cellulose ester,[21] and PHB/PBSU blends were partially miscible; PHB/PCL[15] PHB/PEP[20] blends was found to be immiscible.

Blending PHB with aforementioned various polymers could improve its tenacity, but the cost of these polymers is high and its properties did not meet the requirement. As a result, it is difficult to apply the current PHB blend systems to the industry. Therefore, it is very significant to find a new blend system that satisfies the aforementioned objectives.

Poly(propylene carbonate) (PPC) from CO_2 and epoxy propane is a practical and new biodegradable polymer because of its terminal hydroxyl groups

Correspondence to: P. Hu (hspinghu@mail.tsinghua.edu.cn).

and low cost, as well as its being not harmful to the environment. Furthermore, PPC is an amorphous polymer, with about 40–50% of units in the PPC copolymer chain being carbonate.[23] Recently, some efforts have been invested to apply PPC as plasticizer for rubber or thermoplastics, and surfactant.[24–27] Only a few studies have been reported on blend systems composed of PPC and other polymers, as the crystallization behavior of PHBV/PPC (30/70) melt blend was investigated. PHBV/PPC melting blend had a certain extent of transesterification reaction, and the crystallinity and linear growth rate of spherulites of PHBV could decrease by the addition of PPC.[28]

The blend of PHB and PPC is a biodegradable polymer system, and it has much potential applications in the field of medical and packing materials. However, to the best of our knowledge, no attention has been paid to the blending of PHB and PPC. In this article, the miscibility, the crystallization behavior, the morphology, and mechanical properties of the PHB/PPC blend system with different composition were investigated systematically.

EXPERIMENTAL

Materials

PPC (M_w, 8.5×10^4) was supplied by Changchun Institute of Applied Chemistry, Chinese Academy of Science (Jilin, Changchun), and its commercial products made in Mengxi group (NeiMeng); PHB (M_w, 1.9×10^5) samples used in this study were supplied by NianTian Co. (JiangSu, Nantong). Purification of PPC and PHB was by precipitation from chloroform solution. The M_w of PHB was determined by intrinsic viscosity measurement using the relationship $[\eta] = 1.8 \times 10^{-4} M_w^{0.78}$ [29] in chloroform at 30°C.

Preparation of samples

The PHB/PPC blends were prepared by dissolving both polymers in chloroform ($CHCl_3$, 6.7% w/v). The solutions were cast onto the Petri dishes (100 mm) and evaporated at room temperature overnight to remove the solvent. Finally, the blends were dried in vacuum at 40°C for 24 h and then kept in a desiccator. The blends were prepared in this way with various compositions ranging from PHB/PPC 100/0 to 0/100 in weight ratio.

Measurements

Differential scanning calorimetry

Differential scanning calorimetry (DSC) was performed to study miscibility and thermal behavior of the blends on a Shimadzu DSC-60 TA Instruments equipment. The experiments were performed according to the following program:

RUN 1:
- First heating: heating rate of 20°C min^{-1} from 30 to 190°C for 2 min;
- Cooling: cooling rate of 20°C min^{-1} to 30°C;

The melting point temperature (T_{m1}) and heat of fusion (ΔH_{f1}) for crystals formed during solvent casting stage were measured by the test scan (Run 1).

RUN 2:
- Second heating: heating rate of 20°C min^{-1} from 30 to 190°C for 2 min;
- Cooling: rapidly quenched to −60°C by liquid nitrogen;

T_{m2} and ΔH_{f2} for crystals formed during heating stage were measured.

RUN 3:
- Third heating: heating rate 20°C min^{-1} to 190°C;

the glass transition (T_g) and the cold crystallization temperature (T_{cc}) were measured.

The T_{m1}, T_{m2} and T_{cc} were taken as the peak value of the respective endothermal or exothermal processes in the DSC curves. In the presence of multiple endothermal peaks, the maximum peak temperature was taken as the T_m. The T_gs were obtained by drawing the intersection of the tangent to specific heat increment with the baseline of the high temperature side. All DSC curves were normalized with respect to the sample mass.

Fourier transform infrared spectroscopy

Fourier transform infrared spectroscopy (FTIR) spectra were recorded on a Nicolet 560 FTIR spectroscope. All spectra were recorded at room temperature with 32 scans, at a resolution of 2 cm^{-1}.

Wide angle X-ray diffraction

Wide-angle X-ray difraction (WAXD) experiments were performed with a D/MAX-RB X-ray difractometer using Cu Kα X-ray, with a voltage of 40 kV and a current of 80 mA.

Polarizing optical microscopy

A polarizing optical microscope (POM; BH-2, Olympus) equipped with a hot stage was used to investigate the spherulitic morphology and growth of PHB/PPC blends. Samples cut from the casting films were first heated to 200°C, and then cooled rapidly to 60°C, and allowed to crystallize isothermally.

TABLE I
Thermal Properties of PHB, PPC, and PHB/PPC Blends in the Heating Runs from DSC Measurements

	Run 1[a]			Run 2[b]			Run 3[c]	
Sample composition	T_{m1} (°C)	ΔH_{m1} (J g^{-1})	χ_{c1} (%)	T_{m2} (°C)	ΔH_{m2} (J g^{-1})	χ_{c2} (%)	$T_{g(PHB)}$ (°C)	T_{cc} (°C)
PHB	167.1	61.7	42.1	156.7	51.1	34.8	1.9	60.0
PHB90/PPC10	162.3	54.6	41.4	156.5	45.3	34.3	1.5	53.0
PHB80/PPC20	160.6	48.6	41.4	155.8	38.0	32.4	1.3	52.3
PHB70/PPC30	160.0	41.2	40.1	156.8	36.3	35.4	1.1	54.2
PHB60/PPC40	163.0	35.4	40.2	155.9	29.0	32.3	1.4	53.3
PHB50/PPC50	164.8	30.9	42.2	154.7	15.3	20.9	2.7	55.7
PHB40/PPC60	156.2	21.6	36.8	155.3	20.2	34.3	1.8	58.5
PHB30/PPC70	150.1	12.3	28.0	150.2	6.7	15.2	16.8	40.9
PHB20/PPC80	150.3	7.7	26.3	–	–	–	21.0	–
PHB10/PPC90	–	–	–	–	–	–	24.4	–
PPC	–	–	–	–	–	–	26.6	–

[a] Obtained from original samples formed during solvent evaporation.
[b] Obtained from samples formed during heating stage.
[c] Obtained from samples after DSC cooling run at a rate of 60°C min^{-1}.
–, no results available.
PHB90/PPC10 means, e.g., that the content of PHB in the PHB/PPC blend was 90 wt % and the content of PPC was 10.0 wt %.
T_m, melting temperature; ΔH_m, melting enthalpy, χ_c, crystallinity; T_g, glass transition temperature; T_{cc}, cold crystallization temperature.

Scanning electron micrograph

Scanning electron micrograph (SEM) analysis was performed with a Hitachi S-450 SEM. All specimens were submerged into liquid nitrogen, fractured, and then sputter-coated with a thin layer of gold before SEM observations.

Tensile test procedure

Dumb-bell specimens for mechanical tests were prepared in accordance with ASTM D 638 specification. Tensile properties of samples were determination with a universal test machine (UTM, Instron 5565, Instron) at a cross-head speed of 10 mm min^{-1}. The mean value of at least five specimens of each sample was taken at 25°C.

RESULTS AND DISCUSSION

Analysis of DSC

The DSC studies were conducted to reveal the melting, crystallization behavior, and glass transition of the PHB/PPC blends. The DSC results were recorded in Table I.

Glass transition temperature

Miscibility of PHB/PPC blends on the glass transition temperature (T_g) was investigated by DSC. According to the miscibility between two components, binary polymer blends can be classified into three types: namely completely immiscible, completely miscible, and partially miscible. The miscibility of binary polymer blends can be determined easily by comparison of the T_g of the blends with that of the two components.[12] If binary polymer blends have one single composition-dependent T_g, the two components are completely miscibile in polymer blends. If polymer blends have two composition-independent T_gs close to those of neat components, the two components are completely immiscible polymer blends. If polymer blends have two composition-dependent T_gs, which locate between those of neat components, the two components are partially miscible polymer blends. T_gs of PHB and PPC were 1.9°C and 26.6°C, respectively.

The thermograms of the melt-quenched samples (Run 3) were shown in Figure 1. For PHB/PPC

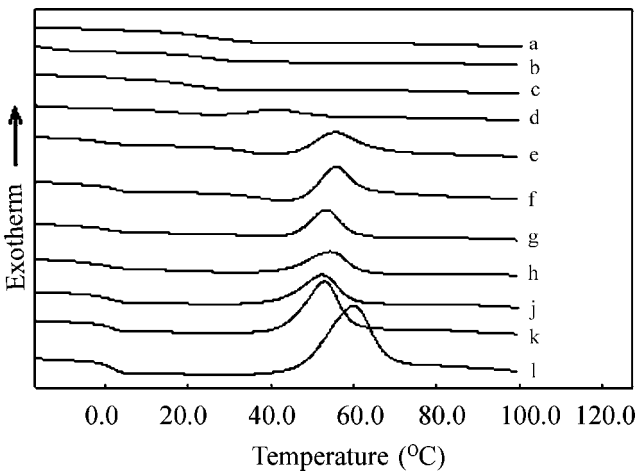

Figure 1 DSC traces of PHB/PPC blends at a heating rate of 20°C min^{-1} (Run 3) after melt quenching. (a) PHB, (b) PHB10/PPC90, (c) PHB20/PPC80, (d) PHB30/PPC70, (e) PHB40/PPC60, (f) PHB50/PPC50, (g) PHB60/PPC40, (h) PHB70/PPC30, (j) PHB80/PPC20, (k) PHB90/PPC10, and (l) PPC.

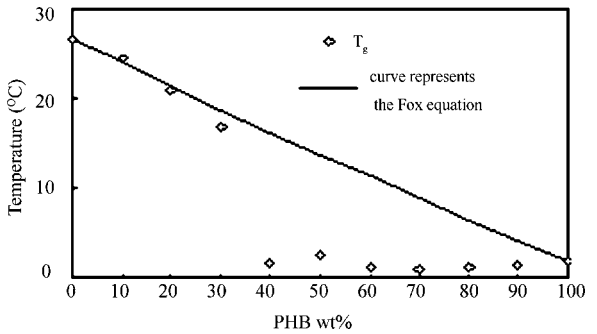

Figure 2 Glass transition temperature of PHB as a function of composition for PHB/PPC blends.

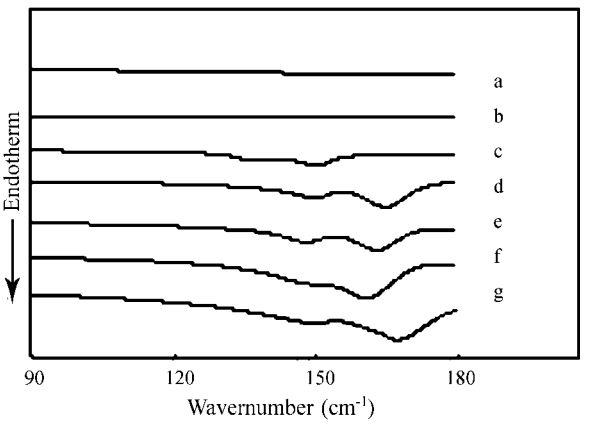

Figure 3 DSC thermograms of solution-casted PHB/PPC blends (Run 1). (a) PHB, (b) PHB10/PPC90, (c) PHB30/PPC70, (d) PHB50/PPC50, (e) PHB60/PPC40, (f) PHB80/PPC20, and (g) PPC.

blend with PHB more than 40 wt %, only one T_g was observed, and its value was close to that of pure PHB. This suggested that an amorphous PHB phase is present in quenched blends. For the blend system, as observed in melt-quenched pure PHB,[30] the glass transition is followed by an exothermic cold crystallization phenomenon, and this cold crystallization peak shifted to lower temperature with an increase of PPC content. Comparing the T_gs of the pure PPC and PPC-rich blends, an endothermic baseline shift associated with the glass transition is observed; especially, for blends with PHB less than 30 wt %, with increasing PHB content in the blend, the T_g decreases and the transition was seen to broaden on the low temperature side.

T_g of the PHB/PPC blend, taken from the curves of Figure 1, was plotted in Figure 2 as a function of the blend composition. It is seen that there is a strong dependence of the measured T_g on the composition of PPC-rich blends. The line drawn through these data points was calculated using the Fox equation[31]:

$$\frac{1}{T_g} = \frac{W_1}{T_{g1}} + \frac{W_2}{T_{g2}} \quad (1)$$

where W denotes weight fraction, and subscripts 1 and 2 indicate the two polymers.

The fact that the T_gs of the blends with 10–30 wt % PHB follows the predictions of the Fox equation is a good indication that the system is completely miscible over this composition range. However, as the PHB content in the system is increased, the variation of T_g was seen to level-off quite noticeably. In fact, the blends containing more than 30 wt % PHB have nearly a constant T_g located in proximity to the T_g of PHB, and this indicates that PHB and PPC are immiscible in blends with PHB content $\geq$ 30 wt %.

Melting temperature

Table I showed the first scan melting temperature (T_{m1}s) of the PHB/PPC cast films (Run 1), as shown in Figure 3. The T_{m1}s of blends are lower than that of pure PHB (Fig. 4). These results are possibly related to the depression of the spherulite crystal size of PHB because of the addition of the PPC in the process of solvent evaporation.

In Run 2 of DSC measurements, for the crystals formed during heating stage, the T_{m2}s of PHB in the blends with PHB $\geq$ 40 wt %, are nearly independent of blend composition and appeared at about 156°C, respectively. However, for the blends containing PHB30 wt %, the addition of PPC almost at the same time causes a substantial depression in the T_{m1} and T_{m2} value of PHB. Even the melting peak of PHB could not be observed for PHB/PPC 10/90 blend. This in itself confirms that there is miscibility between the two components in the amorphous regions.

The T_ms observed here are not equilibrium melting points and not those of samples crystallized isothermally. Considering that all the samples have the same thermal history, the independence of T_m value

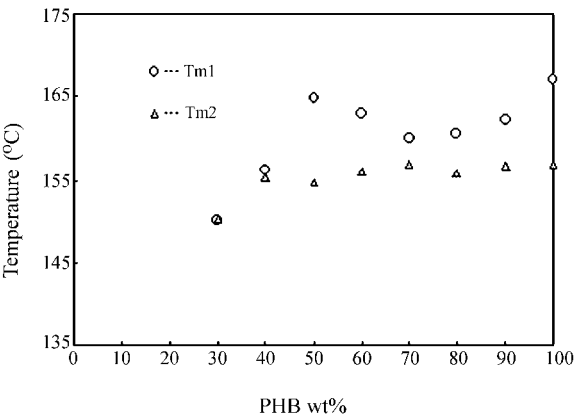

Figure 4 Melting temperature of PHB/PPC blends: T_{m1}, melting peak for crystals formed during solvent-casting stage; T_{m2}, melting peak for crystals during heating stage.

on blend composition should indicate the independence of equilibrium point on composition. By analyzing the earlier melting temperature, we can conclude that there was some interaction between the two components in the PHB/PPC blends with PHB content $\leq$ 30 wt %, which was well-consistent with the conclusion derived from the T_g measurements that the two kinds of blends are miscible.

Cold crystallization temperature

In Run 3, all the cold crystallization temperature of PHB (T_{cc}s) in the blends containing PHB $\geq$ 40 wt % appear at temperature of 55°C $\pm$ 3°C, and they are obviously lower than the pure PHB (60°C; see Table I). In particular, for the blend with PHB content 30 wt %, T_{cc} dropped about 20°C. Unlike the pure PHB, the blends of PHB/PPC 20/80 and 10/90 did not display cold crystallization peaks in the DSC measurement of Run 3.

Melting enthalpies

Table I shows the relationship between the melting enthalpies of blend and PHB content, respectively. The melting enthalpy ΔH_{m1} increases with increase of PHB content in the blend films. Similar results for ΔH_{m2} are obtained in Run 2, except for the blend PHB/PPC 50/50.

Crystallinity of PHB

Table I also showed the crystallinity (χ_cs) of PHB in the blends. The χ_c of PHB phase can be calculated by the following equation:

$$\chi_c = \frac{\Delta H_m}{\Delta H_m^0 \times W_{\mathrm{PHB}}} \quad (2)$$

where ΔH_m, ΔH_m^0, and W_{PHB} represent the melting enthalpy of blend corresponding to PHB, thermodynamic melting enthalpy per gram of PHB (146.6 J g^{-1}),[32] and W_{PHB} is the weight content of PHB in the blend, respectively.

For the PHB/PPC cast films, the change of the crystallinity (χ_{c1}) is inconspicuous with decrease of PHB content in the blends, and χ_{c1} remains above 40% for the blends with PHB $\geq$ 50 wt % (Table I), while χ_{c1} decreased obviously for the blends containing PHB 30 and 20 wt %, which may be attributable to the elution effect of PPC phase. The results of DSC experiment indicate that the crystallization of PHB is suppressed by blending with abundant PPC, consistent with the X-ray results given later. Similar results for the crystallinity of melting blends (χ_{c2}) were also obtained. At the same time, these results also indicate that the PPC phase has some effect on the crystallization kinetics of PHB phase over this PHB content range.

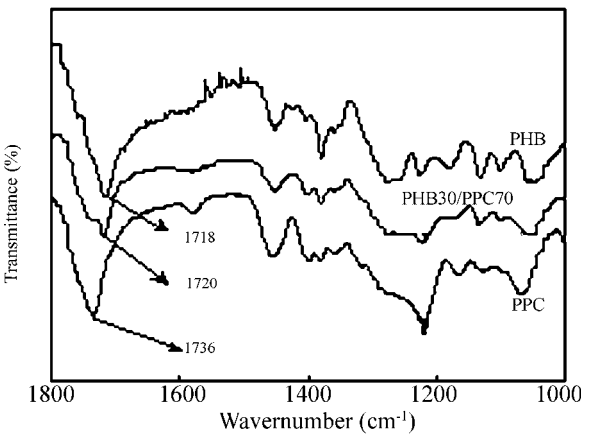

Figure 5 FTIR spectra of PHB, PPC, and PHB30/PPC70 blend. The spectra were collected in the region of 1800–1000 cm^{-1}.

Analysis of FTIR

FTIR was used to examine the possible interaction between the two components. Figure 5 showed the FTIR spectra of pure PHB, pure PPC, and PHB/PPC 30/70 cast film. The C=O stretching bands of PHB are located at 1718 cm^{-1}, with shoulders at about 1740 cm^{-1}, which are representative of PHB crystalline and amorphous zones. C=O stretching bands of PHB/PPC 30/70 cast film and pure PC were at 1720 and 1736 cm^{-1}, respectively. The fact that the C=O stretching bands of blend shifted to a higher wave number showed that between PHB and PPC there exist some interaction. The certain interaction between PHBV and PPC was confirmed in the melting blend PHBV/PPC 30/70.[24] The change trends of FTIR spectra of PHB/PPC blend are similar to that of PHBV/PPC blend.

Analysis of WAXD

The WAXD patterns of PHB, PPC, and PHB/PPC blends films with different composition were shown in Figure 6. The patterns of PHB/PPC (PHB $\geq$ 20 wt %) exhibit well-discriminated diffraction peak raised from the crystallization of PHB, centered at 2θ equal to 13° and 17°. It is obvious that the position of the diffraction peaks remains unchanged, which implies that the addition of PPC did not result in any change of the crystalline structure of PHB. The intensities of the diffraction peaks decreased with increasing PPC content, and no obvious diffraction peak appeared in the spectra of PHB/PPC 10/90.

Besides hydrogen-bonding interaction, the possible factor that lowers the degree of crystallinity of PHB was the difference in the glass transition temperature

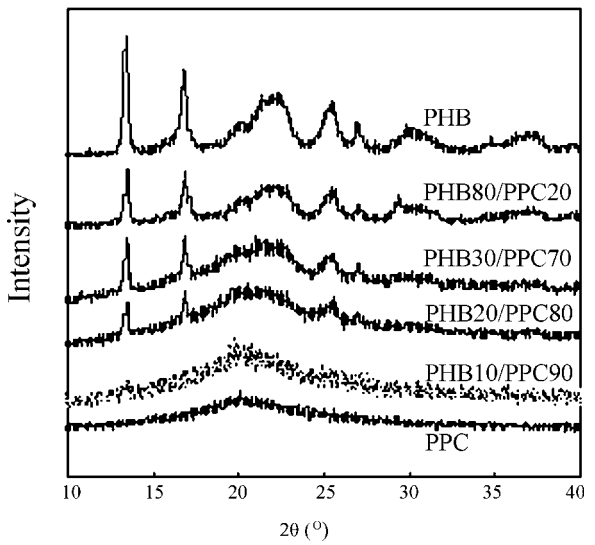

Figure 6 WAXD of the films of PHB, PPC, and PHB/PPC blends films at room temperature.

(T_g) between PHB and PPC. The crystallization temperature (room temperature) is lower than T_g of PPC (26.6°C), but is higher than that of PHB (about 1.9°C). Hence, PHB molecules in the amorphous phase are probably trapped by the ''glassy'' PPC environment, as PHB and PPC are compatible in the amorphous phase. Furthermore, the DSC data indicated that the crystallization of PHB was suppressed by blending with PPC, and PHB melting peak was not observed for the blend PHB/PPC 10/90; therefore, the earlier WAXD results are consistent with the DSC results.

Analysis of POM

The micrographs of isothermal crystallization of PHB, PPC, and their blends were obtained by POM. From Figure 7, the well-defined spherulites were found growing rapidly at 60°C for pure PHB. In the case of PHB/PPC 50/50 blend, PHB can also crystallize according to a spherulitic morphology, and large spherulites are observed. In the blends containing PPC 80 wt %, no large spherulite was observed. Meanwhile, no clear optical evidence of phase separation in the melting was found for PHB/PPC 30/70, 20/80, and 10/90 blends. This indicated that PHB shows miscibility with PPC to some extent for this composition at least on the level of the observation scale. Moreover, for the blend PHB/PPC10/90, there was no spherulite of PHB to be found. This was identical with the phenomena observed under nonisothermal processes.

These results are related to the depression of the spherulite growth rate of PHB because of the dilution effect of the PPC component. However, this effect should not prevent PHB from crystallizing completely during nonisothermal crystallization runs, especially at a lower cooling rate (such as 20°C min^{-1}). The melting miscibility on the primary nucleation processes should also be taken into account. The aforementioned crystallization behavior can be explained only on the assumption that PHB crystallizes from a mixed phase, where the macromolecules of the two species are intimately intermingled.

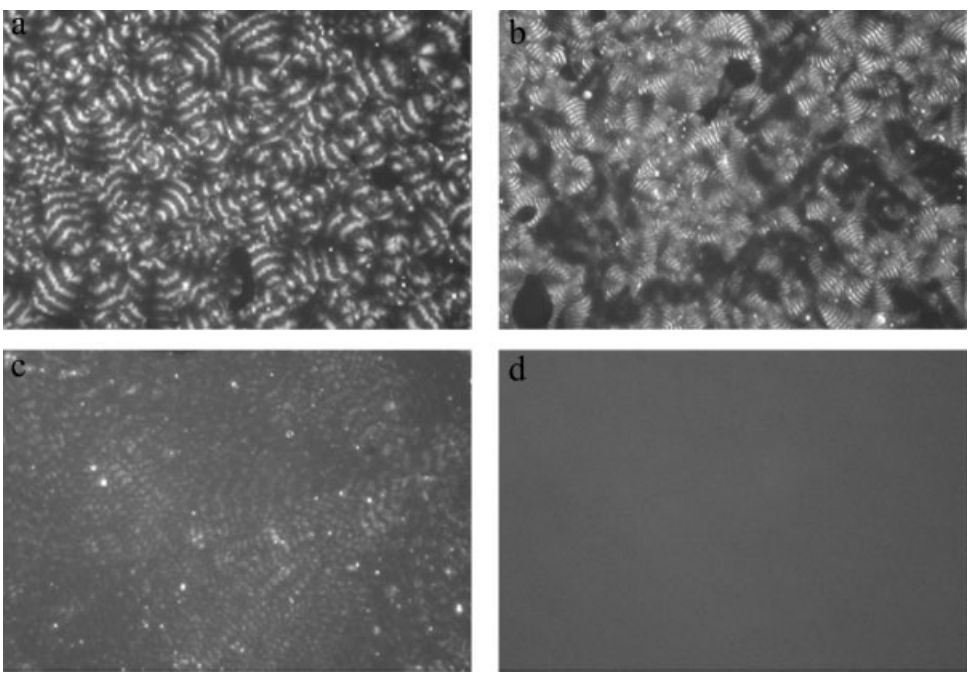

Figure 7 Polarizing optical micrographs of PHB, PPC, and PHB/PPC blends under crossed polar (same magnification, magnification factor 100). (a) PHB, (b) PHB50/PPC50, (c) PHB20/PPC80, and (d) PHB10/PPC90.

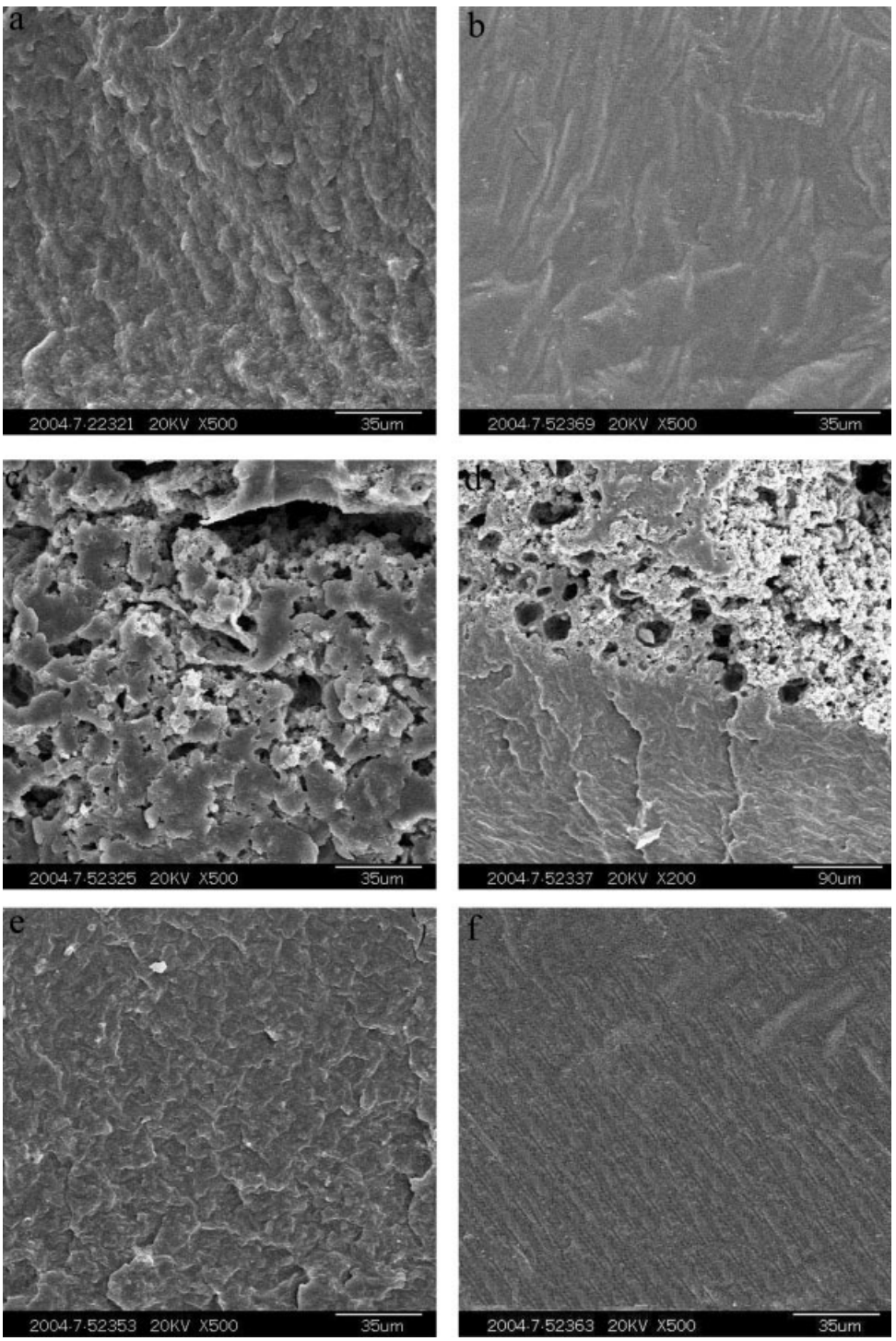

Figure 8 Scanning electron micrographs of PHB, PPC, and its blends. (a) PHB, (b) PPC, (c) PHB80/PPC20, (d) PHB50/PPC50, (e) PHB30/PPC70, and (f) PHB10/PPC90.

Analysis of SEM

Examination of the surfaces of fractured films obtained from solution-cast PHB/PPC blends was carried out using SEM (Fig. 8). Before analyzing the morphology of blends, fractured surfaces of both parent polymers were studied. The freshly fractured surface of PHB film is chaotic and exhibits a bristled openwork polymeric network [Fig. 8(a)]. On the other hand, the fractured surface of PPC film is smooth and only a few bellows [Fig. 8(b)]. Figure 8(c–e), and f showed the fractured surface of 80/20, 50/50, 30/70, and 10/90 PHB/PPC blends. The higher the PHB content, the rougher the surface of fracture appears. By comparison of these micro-

TABLE II
Mechanical Properties of PHB/PPC Cast Films

Sample (PHB/PPC)	Tensile strength (MPa)	Ultimate strain (%)	Modulus of elasticity (MPa)
40/60	5.5	2.7	405.4
30/70	4.8	305.4	100.2
20/80	3.4	391.1	7.9
10/90	2.6	1000.0	5.6
0/100	2.0	1089.3	2.1

graphs, it seems that this phenomenon could be due to the phase separation between PHB and PPC. In Figure 8(c), the bristled openwork PHB network is easily seen, and the network size and distribution are very irregular. This is an indication that PHB and PPC form mainly a two-phase system. Increasing the PPC content induced an increase of the appearance of smooth polymeric domains. For PHB/PPC 50/50 composition, a distinct phase separation structure was seen. However, for the PHB/PPC blend containing PHB $\leq$ 30 wt % [Fig. 8(e,f)], the blend tended to form a more compact film. The differences observed in the morphology between pure polymer and blends could be discussed from the crystallinity properties. The crystallization rate of blends is slower than that of the pure PHB cast films from solution. The blends could not crystallize in the elapsed time in which evaporation of solvent occurs, and consequently they form a complete amorphous film at this initial step. After chloroform evaporation, the spherulites with different crystallite size and distribution may be formed through PPC, with the subsequent impact into the amorphous phase.

Tensile test

The results of tensile test were listed in Table II. PHB displays a brittle behavior, and PHB-rich samples (up to 50 wt %) were very brittle and break into fragment in the process of preparation samples for tensile test. For PPC-rich samples, the brittleness of PHB was improved apparently by blending with PPC. The elongation at break of PHB was improved significantly in the blends while the tensile strength decreased slightly, and modulus of elasticity of blends decreased with increase of PPC content.

CONCLUSIONS

Blends consisting of PHB and PPC prepared by solution blending were processed using chloroform as a common solvent. The miscibility, crystallization, melting behavior, morphology, and mechanical properties of PHB/PPC blends were investigated by using DSC, FTIR, WAXD, POM, and SEM. The following conclusions were obtained.

PHB was found to show miscibility with PPC for PHB/PPC 30/70, 20/80, and 10/90 blends from the change in the glass transition temperature, the depression of the equilibrium melting point temperature of PHB, and the decrease in the crystallization temperature of PHB and POM observation. And the crystallization of PHB was suppressed by blending with abundant PPC (PPC $\geq$ 40%). When PPC content was more than 90 wt %, no spherulitic was observed. However, PHB showed immiscibility with PPC for the blends with PHB content greater than 40%, as shown by the existence of unchanged composition independent glass transition temperature. And the crystallization behavior of PHB did not possess significant changes, and SEM observation also showed a clear phase separation. The elongation at break of PHB was improved significantly in the blends while the tensile strength decreased slightly.

References

1. Howells, E. R. Chem Ind 1982, 15, 508.
2. King, P. P. J Chem Technol Biotechnol 1982, 32, 2.
3. Holmes, P. A. Phys Technol 1985, 16, 32.
4. Greco, P.; Martuscelli, E. Polymer 1989, 30, 1475.
5. Kumagai, Y.; Doi, Y. Polym Degrad Stab 1992, 36, 241.
6. Lotti, N.; Pizzoli, M.; Ceccorulli, G. Polymer 1993, 34, 4935.
7. Yang, H.; Li, Z. H.; Qian, H. J. Polymer 2004, 45, 453.
8. Avella, M.; Martuscelli, E.; Greco, P. Polymer 1991, 32, 1647.
9. Kumagai, Y.; Doi, Y. Polym Degrad Stab 1992, 35, 87.
10. Avella, M.; Martuscelli, E.; Raimo, M. Polymer 1993, 34, 3234.
11. Yoichiro, A.; Naoko, Y.; Minoru, S. Polymer 1992, 33, 4763.
12. Zhao, B. Q.; Takayuki, I.; Toshio N. Polymer 2003, 44, 2503.
13. Koyama, N.; Doi, Y. Polymer 1997, 38, 1589.
14. Tsuyoshi, F.; Harumi, S.; Rumi, M. Polymer 2007, 48, 1749.
15. Lisuardi, A.; Schoenderq, A.; Gada, M. Polym Mater Sci Eng 1992, 67, 298. Proceedings of the ACS Division of Polymeric Materials Science and Engineering.
16. Organ, S. J.; Barham, P. J. Polymer 1993, 34, 459.
17. Dave, P. B.; Ashar, N. J.; Gross, R. A. Am Chem Soc 1990, 31, 442.
18. Satoh, H., Yoshie, N.; Inoue, Y.; Polymer 1994, 35, 286.
19. Chen, C.; Dong, L. S.; Peter, H. F. Y. Eur Polym J 2006, 42, 2838.
20. Juliana, A. L.; Maria, I. F. Eur Polym J 2006, 42, 602.
21. Giuseppina, C.; Maria, P.; Mariastella, S. Macromolecules 1993, 26, 6722.
22. Ikejma, T.; Inoue, Y. Carbohydr Polym 2000, 41, 351.
23. Zhao, X. J.; Liu, B. Y.; Wang, X. H.; Zhao, D.; Wang, F. Methods of rare earth complexes portfolio catalyst. CN98125654, 1998.
24. Huang, Y. H.; Yang, X. H.; Zhao, S. L.; Lin, G. J Appl Polym Sci 1998, 61, 1479.
25. Wang, S. J.; Huang, Y. H.; Cong, G. M. J Appl Polym Sci 1998, 63, 1107.
26. Huang, Y. H.; Wang, J. Z.; Liao, B. J Appl Polym Sci 1997, 64, 2457.
27. Pang, H.; Liao, B.; Huang, Y. H. J Appl Polym Sci 2002, 86, 2140.
28. Li, J.; Liu, J. J. Chem J Chin Univ 2004, 2, 1145.
29. Akita, S.; Einaga, Y.; Miyaki, Y. Macromolecules 1976, 9, 774.
30. Scandola, M.; Pizzoli, M.; Ceccorulli, G.; Paoletti, S.; Navarini, L.; Cesaro, A. Int J Biol Macromol 1988, 10, 373.
31. Fox, T. G. Bull Am Phys Soc 1956, 2, 123.
32. Barham, P. J.; Keller, A.; Otun, E. L.; Holmes, P. A. J Mater Sci 1984, 19, 2781.